Landslide Susceptibility Estimated From Mapping Using Light Detection and Ranging (LIDAR) Imagery and Historical Landslide Records, Seattle, Washington

By William H. Schulz

U.S. Geological Survey Open-File Report 2005–1405

U.S. Department of the Interior
U.S. Geological Survey

U.S. Department of the Interior
Gale A. Norton, Secretary

U.S. Geological Survey
P. Patrick Leahy, Acting Director

U.S. Geological Survey, Reston, Virginia 2005

For product and ordering information:
World Wide Web: http://www.usgs.gov/pubprod
Telephone: 1-888-ASK-USGS

For more information on the USGS—the Federal source for science about the Earth,
its natural and living resources, natural hazards, and the environment:
World Wide Web: http://www.usgs.gov
Telephone: 1-888-ASK-USGS

Schulz, W.H., 2005, Landslide susceptibility estimated from mapping using light detection and ranging (LIDAR) imagery and historical landslide records, Seattle, Washington: U.S. Geological Survey Open-file Report 2005–1405, 16 p., 1 plate, map scale 1:30,000.

Contents

Figures

Tables

Landslide Susceptibility Estimated From Mapping Using Light Detection and Ranging (LIDAR) Imagery and Historical Landslide Records, Seattle, Washington

By William H. Schulz

Abstract

Landslides have resulted in significant losses in Seattle, Washington, since at least the 1890s. A basic tool for assessing regional landslide hazards is a landslide inventory map, which shows the distribution of known landslides, assists in understanding landslide processes, and can be used to estimate landslide susceptibility. Previous landslide inventory maps of Seattle provide locations of some landslides but fail to delineate most areas of historical landslide activity. Recently, light detection and ranging (LIDAR) data were used to map Seattle landslides and landslide headscarps. That mapping effort identified about 4 times as many landslides as had been identified in previous inventories. The present study attempts to characterize landslide susceptibility of the Seattle area based on a recent LIDAR-based map of landslides and records of historical landslides. The spatial distributions of the LIDAR-mapped landslides, headscarps, and denuded slopes were evaluated with respect to the distribution of over 1,300 historical landslides. About 93 percent of the historical landslide locations lie within the boundaries of the LIDAR-mapped landforms. Virtually all (99.7 percent) of the historical landslides that initiated only from natural causes lie within these boundaries. The spatial densities of historical landslides within each landform were determined, as were the densities of historical landslides with specific characteristics. These densities represent relative landslide susceptibilities of the landforms and are portrayed in map form. The map shows the landforms as susceptibility zones and provides estimates of susceptibilities to deep and shallow landslides, falls, flows, landslides with long runout, and large and small landslides. The susceptibility map also successfully delineates areas of historical landslide activity. Therefore, the susceptibility map appears to be far more useful and versatile in estimating and characterizing future landslide activity than are typical landslide susceptibility maps. Notably, 88 percent of historical landslides in Seattle are at least partly caused by human activity. Consequently, the spatial distributions and densities of human-caused landslides also were determined and evaluated. Since these landslides are human caused and relatively abundant, they may be most easily addressed by landslide-hazard mitigation efforts.

Introduction

Landslides are common in the Seattle, Washington, area (fig. 1) and have caused significant property damage and human casualties (for example, Gerstel and others, 1997; Paegeler, 1998). Perhaps the most basic tool for reducing regional landslide hazards is a landslide inventory map. Landslide inventory maps identify landslides and provide information necessary for evaluating conditions responsible for landslide formation on a regional basis. Several landslide inventory maps have been constructed for Seattle using aerial photographs, topographic maps, historical landslide reports, and field-based studies (Waldron and others, 1962; Waldron, 1967; Youngmann, 1979; Yount and others, 1993; Wait, 2001). However, evaluation of these maps with respect to a georeferenced database containing about 1,400 historical landslides (Shannon & Wilson, Inc., 2003) indicates that most historical landslides occur in areas not shown as landslides on the inventory maps. The primary reason for the lack of successful delineation of most of Seattle's landslide-prone areas in the inventory maps probably is that it is very difficult to identify landslides and landslide-prone landforms through the dense canopy of vegetation present in the region. This difficulty has been addressed recently through acquisition of light detection and ranging (LIDAR) data, which provide a much more accurate representation of the ground surface in forested areas than is possible by using photogrammetric methods. A LIDAR-derived digital elevation model (DEM) was recently used to map about 400 percent more landslides in Seattle than had been mapped previously (Schulz, 2004). Figure 2 illustrates the ability of LIDAR data to reveal geomorphic ground-surface characteristics indicative of landslides. As is the case for most of Seattle, the large landslide shown in figure 2 is actually a landslide complex that includes many individual landslides that range in volume from tens to thousands of cubic meters. Complexes such as this commonly include several types of Seattle landslides (based on evaluation of the database of historical landslides; Shannon & Wilson, Inc., 2003).

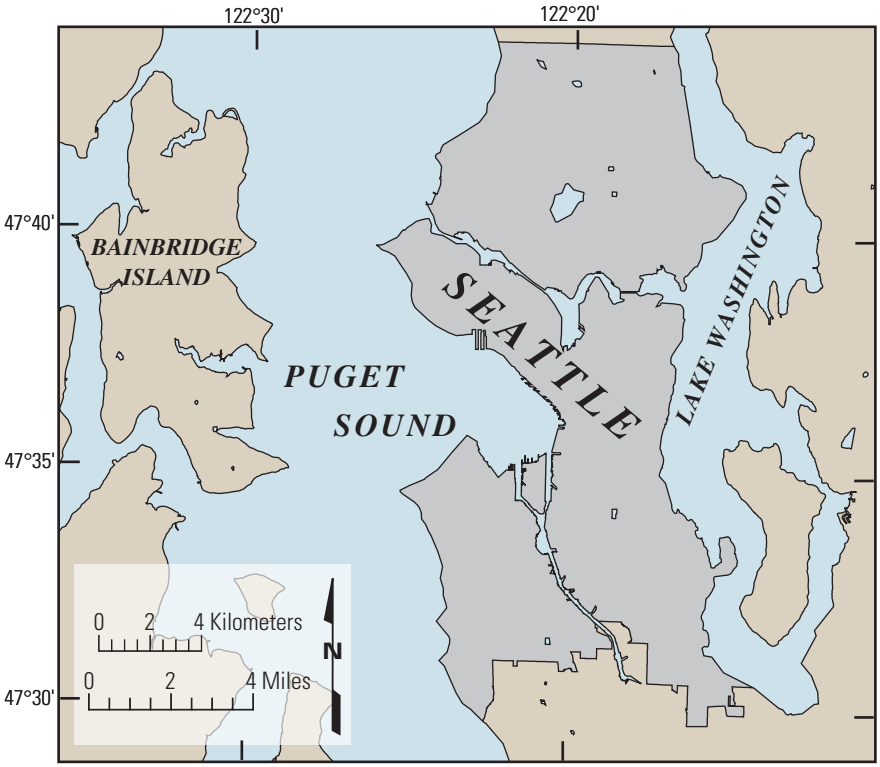

Figure 1. Map showing the location of Seattle, Washington (gray area), in relation to Puget Sound, Lake Washington, and Bainbridge Island.

The study described in this paper sought to identify spatial relations between the LIDAR-mapped landslides, most of which are largely prehistoric features (Schulz, 2004), and historical landslides. However, the LIDAR-based landslide map (Schulz, 2004) includes only landslide deposits and associated headscarps; it does not include landslide scars or cavities. A significant number of slopes in Seattle appear to have been formed by erosion and landsliding as indicated by apparent landslide scars and cavities, but lack identifiable landslide debris in the LIDAR imagery. In the present study, the LIDAR-based landslide map was modified to include all landforms interpreted to have been created primarily by landsliding, including slopes on which landslide deposits were not identified. The spatial distributions of the LIDAR-mapped landforms were subsequently evaluated with respect to the distribution of historical landslides (Shannon & Wilson, Inc., 2003). Strong relations were identified between these data sets and were used to create a relative landslide susceptibility map of Seattle. The map provides the relative susceptibilities to large, small, shallow, and deep landslides, landslides with long runout, falls, and flows for the different landform types. Spatial distributions of human-caused landslides and the LIDAR-mapped landforms also were evaluated and provide insight into the adverse impacts that human activities have on slope stability and how those impacts can be reduced.

Background of Seattle Landslides

The topography and geology of Seattle primarily result from a series of Late Pleistocene glacial and interglacial cycles, although Tertiary bedrock crops out extensively in the southeastern part of the city (Waldron and others, 1962; Mullineaux and others, 1965; Galster and Laprade, 1991; Booth and others, 2000; Kathy G. Troost, Pacific Northwest Center for Geologic Mapping Studies, written commun., 2003, 2004). Holocene fluvial and coastal processes and human activity have locally modified Pleistocene landforms. Seattle occupies an isthmus between Puget Sound and Lake Washington (fig. 1), and its topography is characterized by glacially sculpted uplands with steeper slopes along coastlines and drainages that formed through erosion and mass-wasting processes (pl. 1, fig. 2). Bluffs occur along much of the current Puget Sound and Lake Washington coastlines, as well as along former coastlines such as the perimeter of the filled Interbay area and the northwestern part of Beacon Hill (pl. 1). The bluffs result from coastal erosion that has accompanied sea-level rise since retreat of the last continental glacier from the region about 13,600 years ago (Downing, 1983; Booth, 1987; Terich, 1987). Formation and retreat of Seattle's coastal bluffs has been accomplished primarily by erosion due to wave action and landsliding (Galster and Laprade, 1991; Hampton and others, 2004).

2A

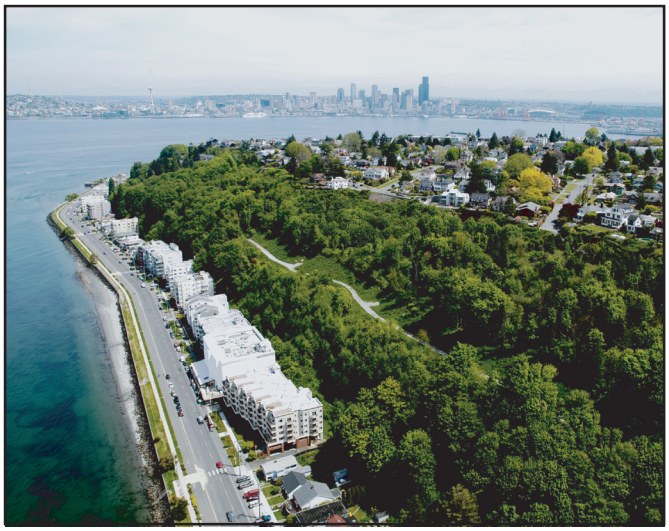

2C

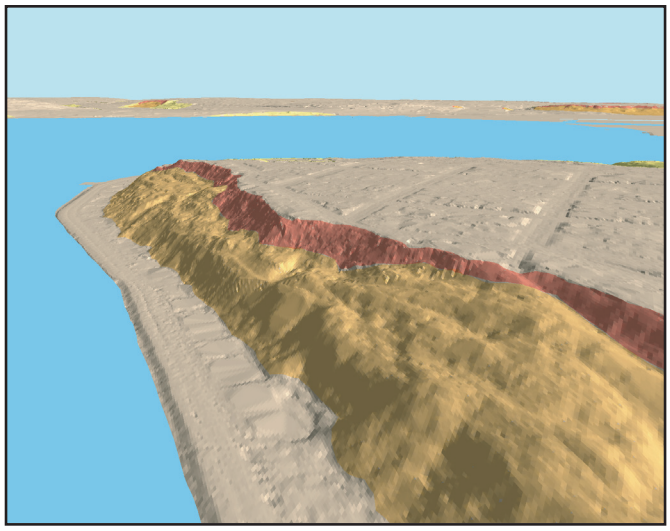

2B

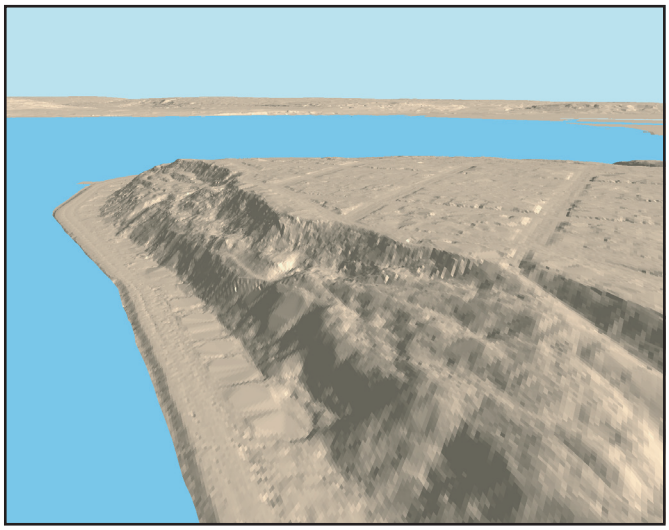

Figure 2. Oblique aerial views of part of West Seattle toward the northeast and Duwamish Head (pl. 1).
A, Photograph courtesy of Shannon & Wilson, Inc., Seattle;
B, LIDAR-derived, bald-earth DEM with no vertical exaggeration and a virtual sun at an azimuth of 180° and 30° above the horizon;
C, LIDAR-derived DEM of fig. 2*B* with landslide deposits shown in orange and headscarps shown in red.
Hummocky topography indicative of landslide debris and steep headscarps are visible in the LIDAR imagery (2*B* and *C*), and less so in the aerial photograph (2*A*). The truncation of the relatively smooth, flat, glacially sculpted uplands by landslides situated along surface water bodies also is apparent on the figure.

Seattle landslides are concentrated along the coastal bluffs, but also occur on hillslopes along drainages and on steep, glacially sculpted landforms (Waldron and others, 1962; Waldron, 1967; Tubbs, 1974; Youngmann, 1979; Yount and others, 1993; Harp and others, 1996; Gerstel and others, 1997; Baum and others, 1998; Baum and others, 2000; Laprade and others, 2000; Wait, 2001). The primary long-term process that results in Seattle landslides appears to be erosion of slope toes by surface water (for example, Gerstel and others, 1997); at least 93 percent of LIDAR-mapped landslides occur along slopes adjacent to existing and former surface-water bodies and drainage courses (Schulz, 2004). Other than a small number of human-caused landslides, landslides do not appear to have occurred in Seattle in the absence of slope undercutting by surface water. Apparently, Seattle's glacially sculpted hillslopes do not have great enough inclination for landslides to occur without human modification of natural conditions. This conclusion contrasts with the generally accepted theory proposed by Tubbs (1974, 1975) that most landslides in Seattle are caused by ground-water conditions present near the basal contact of the Vashon advance outwash (Esperance Sand) (for example, Galster and Laprade, 1991; Laprade and others, 2000; Savage and others, 2000; Wait, 2001; Coe and others, 2000; Coe and others, 2004). Tubbs's theory was based on the observation that 40 percent of the largest landslides that occurred during the winter of 1971–72 were located at least partly within a zone 61-meter (m) (200 ft) wide centered on the contact. Whatever the principal long-term slope-destabilizing processes, nearly all of the historical Seattle landslides appear to have finally been triggered by heavy winter precipitation (Tubbs, 1974; Galster and Laprade, 1991; Miller, 1991; Gerstel and others, 1997; Baum and others, 1998; Laprade and others, 2000; Montgomery and others, 2001; Coe and others, 2004). Evaluation of the historical landslide database (Shannon & Wilson, Inc., 2003) indicates that 88 percent of Seattle's historical landslides may have been caused, to some degree, by human activity. This percentage may be erroneously high, however, because landslides in undeveloped areas are rarely caused by human activity and commonly go unreported (Laprade and others, 2000).

Seattle landslides are typically rapid, shallow slides, flows, and falls, as well as generally slower moving, deep translational, rotational, and complex slides of earth and debris (terminology from Cruden and Varnes, 1996) (Tubbs, 1974, 1975; Thorsen, 1989; Galster and Laprade, 1991; Harp and others, 1996; Gerstel and others, 1997; Baum and others, 1998; Baum and others, 2000; Laprade and others, 2000; Montgomery and others, 2001; Coe and others, 2004; Schulz, 2004). The database of historical landslides (Shannon & Wilson, Inc., 2003) indicates that about 72 percent were shallow (less than a few meters thick), 19 percent were deep, 6 percent were flows, and 3 percent were falls. About 85 percent of these historical landslides were small (less than a few meters thick and 930 m^2), while 15 percent were larger than this. About 15 percent of the historical landslides had rapid displacement of more than 15 m (50 ft).

Data and Methods

LIDAR Data

Acquisition and processing of the LIDAR data are described by the Puget Sound LIDAR Consortium (PSLC) on their website (http://pugetsoundlidar.org). The data also are available there. The LIDAR-derived DEM used for the present study was produced by using algorithms to remove data for nonground features (for example, trees, shrubs, buildings, and vehicles) and is commonly referred to as a bald-earth or bare-earth DEM. The DEM has vertical accuracy that typically is on the order of ±30 cm but is considerably worse in some areas. Horizontal accuracy is such that PSLC recommends use of the data at a scale of 1:12,000 or smaller. The DEM is in Washington State Plane projection with English units and has a grid cell size of 1.8 m (6 ft).

Historical Landslide Data

The georeferenced database of historical Seattle landslides was produced by using records of various government agencies and those of Shannon & Wilson, Inc. (Laprade and others, 2000; Shannon & Wilson, Inc., 2003; Coe and others, 2004). The database of historical landslides used in this study (Shannon & Wilson, Inc., 2003) contains records for 1,433 landslides dating back to 1890. Each landslide is represented spatially in the database by a point location that marks the approximate center of its headscarp (the database is described by Laprade and others, 2000). The database only provides relatively accurate (Laprade and others, 2000) locations for 1,308 of the 1,433 landslides, and only records for the 1,308 accurately located landslides were used during the present study. Shannon & Wilson, Inc. (2003) also provides attributes for each landslide for which attributes could be determined; these attributes include date of occurrence, landslide type, size, and potential causes. Of the 1,308 landslides whose locations were determined, 1,273 were of known type, 1,247 were of known size, 1,236 had documented potential causative factors, and 1,214 had known runout characteristics (long-runout landslides are defined as those with greater than 15.2 m [50 ft.] of displacement; Laprade and others, 2000). The historical landslides were segregated by potential human causation during the present study. Landslides with apparent human causes are identified in the historical landslide database as being triggered by human activity, having involved graded slopes, or having other observed human causes.

The historical landslide database has two significant limitations with respect to this study. First, for landslides to be part of the database, they must have been reported. Although this observation may seem trivial, its implications are not. Significant settlement of Seattle began about the beginning of the 20th century and spread to different areas of the city throughout the century, thus areas in which landslides have been reported were settled as early as the 1850s to as late as recently (Galster and Laprade, 1991). Therefore, the spatial and temporal density of reported historical landslides is strongly dependent on settlement and development patterns throughout Seattle. In addition, development of coastal bluffs and slopes along drainages generally is of significantly lower density than that of the glacially sculpted uplands, and a large number of parks have been created along the bluffs and drainages. These factors probably result in a lower reporting frequency (on a per-landslide basis) for the presumably more landslide-prone bluff and drainage-slope areas than for the presumably more stable, densely developed glacial uplands. The database bias, due to these reporting problems, may skew results of any temporal or spatial study. For the present study, however, it is believed that the adverse effects are low because the temporal distribution of historical landslides is not considered, and the spatial distribution is only considered on a landform-by-landform basis. Since landforms used in this study are spread throughout the entire city, whether a given part of the city was developed prior to another is irrelevant. What is relevant is whether each landform in a given part of the city was developed simultaneously and at the same density. As discussed above, landforms in Seattle generally have not been developed at equal densities. The resulting bias in the results of the present study should be toward a greater apparent density of landslides in areas of greater development density, which generally correspond to the areas of probable lower landslide susceptibility (the relatively flat, glacially sculpted uplands). Consequently, the reporting bias causes landslide-prone areas to appear less susceptible to landslides than they are and relatively stable areas to appear more susceptible than they are.

The second limitation of the historical landslide database that could affect results of this study is the representation of landslides as discrete points located at the center of their headscarps. That representation permits identification of only one landform area in which each landslide occurred, while more than one may have been involved. Results of evaluations of the spatial distributions of historical landslides and landforms may be biased in an upslope direction, that is, biased toward the headscarp landform (described below) because of this location representation inherent in the database. It is thought that this bias should be minor for the present study because 85 percent of Seattle landslides are less than about 30 m across (based on small landslides being defined as less than 930 m^2) and 10-m buffers were applied to

the landslide landform prior to the analyses. Therefore, historical landslides that presumably mostly occurred within the landslide landform were identified as such, even though their locations as represented in the database may have placed them within the originally mapped (nonbuffered) boundaries of the headscarp landform.

Mapping Using LIDAR Imagery

Landforms were mapped in a GIS using images derived from the LIDAR DEM. Imagery used for mapping included shaded-relief maps with various virtual sunlight orientations, slope and topographic contour maps, and several hundred topographic profiles. Imagery was evaluated visually during mapping at scales of 1:30,000 to 1:2,000 and landform boundaries generally were mapped at a scale of about 1:5,000. However, the final map is intended to be viewed at a scale of 1:20,000 or smaller. Mapped landforms were evaluated in the field during August 2003.

The three landforms that were mapped are landslides, landslide headscarps, and denuded slopes. Denuded slopes are those slopes that formed by erosion and mass wasting (hence the term "denuded"; see Bates and Jackson, 1987) following deglaciation. Landslides were identified during mapping based on features such as scarps, hummocky topography, convex and concave slope areas, midslope terraces, and offset drainages. Nearly all of the mapped landslides appear to include numerous smaller landslides as indicated by variable ages of vegetation, intersecting headscarps and margins, and variable relative ages of deposits and scarps within a given landslide area. Landslides and headscarps were only mapped where both could be identified for a given landslide area; isolated possible headscarps or landslide deposits were not mapped. Denuded slopes were mapped where glacial landforms are truncated by slopes formed by postglacial erosion and mass wasting, but where extensive landslide deposits and associated headscarps could not be identified. In most cases, denuded slopes appear to consist of intersecting landslide scars of differing ages and lack or have only very thin, overlapping landslide deposits located low on slopes. Field observations indicate that most denuded slope areas have thin landslide deposits that generally are not discernible in LIDAR imagery because many Seattle landslides are too small and thin to be resolved by LIDAR; furthermore, landslide deposits have often been removed by erosion or man. In some areas, denuded slopes formed adjacent to glacial lakes and outwash streams contemporaneously with glaciation, but were not subsequently overridden by later glacial advances.

In all cases, mapped denuded slopes, landslides, and landslide headscarps truncate glacial landforms; they obviously postdate the youngest stages of glaciation in this region. Figure 2 shows a landslide and headscarp complex along the Puget Sound coastline that truncates relatively flat, glacially sculpted uplands in West Seattle. Figure 3 is an oblique view from the northeast of West Seattle, and it shows several other examples of truncated glacial landforms. These include the linear, north-south trending, glacially sculpted ridges (upper left to lower right in fig. 3) that are clearly truncated by landslides, headscarps, and denuded slopes adjacent to the Duwamish River floodplain, which is located in the left half of figure 3. Another example is the denuded slope, landslide, and headscarp area along the Longfellow Creek drainage, which was the location of abundant surface-water flow in lakes and outwash plains during retreat of the final glacier to occupy the area (Kathy G. Troost, Pacific Northwest Center for Geologic Mapping Studies, written commun., 2003, 2004). Relatively flat, glacially sculpted uplands are similarly truncated around most of the perimeter of West Seattle, as well as inland along drainages, former glacial lake shores, and glacial outwash streams (fig. 3). The morphologic differences between glacially sculpted landforms and landforms that formed following retreat of glacial ice (denuded slopes, landslides, and headscarps) are readily apparent in figures 2 and 3 and in the LIDAR imagery, in general.

Landslides and denuded slopes were mapped as polygon features, and headscarps were mapped as curvilinear features. Following mapping, 10-m buffers were applied to the landslide and denuded slope polygons to account for error in the LIDAR imagery and in mapping, as well as in the locations of historical landslides. A 10-m buffer was applied to the upslope side of headscarps, and a 150-m buffer to the downslope side in order to create a polygon feature for each headscarp. The buffered headscarp polygons then were clipped by the landslide polygons, and the resulting headscarp polygons and landslide polygons were used to clip the denuded slope polygons to produce the final mapped features.

Spatial Relations Between LIDAR-Mapped Landforms and Historical Landslides

Upon completion of the landform map, the landform in which each historical landslide in the database (Shannon & Wilson, Inc., 2003) was situated was determined in a GIS and appended to the historical-landslide attribute table. The table then was used to determine spatial densities of historical landslides by landform, including the densities of various types of historical landslides. These densities ultimately were used to estimate landslide susceptibilities throughout Seattle.

Results

Plate 1 includes a shaded-relief map of Seattle with the mapped headscarp, landslide, and denuded slope landforms. These landforms, and the area outside of them, also are labeled as zones on the plate. Table 1 shows the total area of each of the landforms and the percentage of Seattle land area that they cover. Table 2 provides the spatial densities of historical landslides within each landform as the number of historical landslides per square kilometer. Historical landslides are segregated in the table by type, size, and whether long runout occurred. The densities shown in table 2 are equivalent to the relative susceptibilities of the landforms to past landsliding. Because future landslide activity in Seattle will likely be similar to that of the past (for example, Thorsen, 1989; Baum and others, 1998; Laprade and others, 2000), the densities shown in table 2 should approximate

3*A*

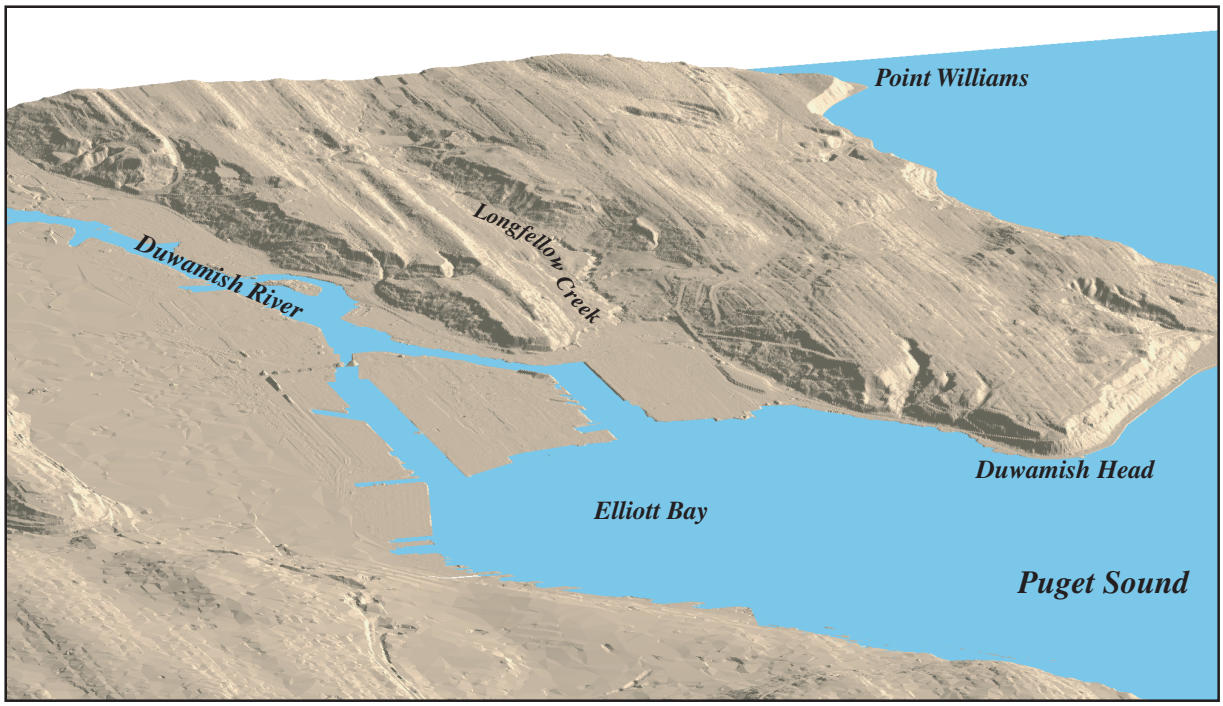

3*B*

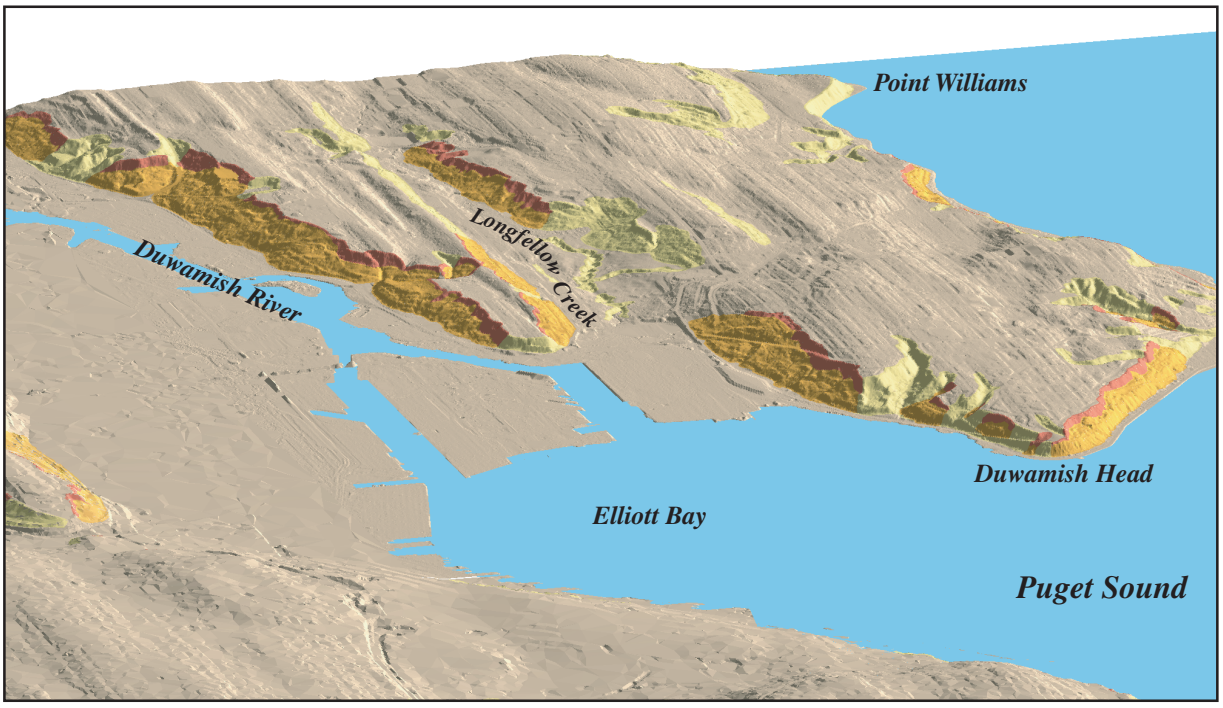

Figure 3. Oblique aerial view of LIDAR-derived, bald-earth DEM of West Seattle (pl. 1). View is from the northeast toward the southwest. Imagery has 1.5 times vertical exaggeration and a virtual sun at an azimuth of 270° and 30° above the horizon. West Seattle is approximately 4.6 km across at the top of the figure.
A, Landforms created by landsliding are visible, for example, adjacent to the Duwamish River floodplain and along the Puget Sound coastline. Glacial landforms include relatively smooth, gently sloping, north-south trending (upper left to lower right in the figure) ridges. Landslide-related landforms generally are hummocky, steeply inclined, and abruptly truncate the glacial landforms along coastlines and drainages.
B, Results of landform mapping using LIDAR are shown draped on figure 3*A*. Landforms shown are landslides (orange), headscarps (red), and denuded slopes (yellow).

Table 1. Areas of the LIDAR-mapped landforms, Seattle, Washington.

Region	Area (square kilometers)	Percentage of total area
Headscarp landform	2.50	1.16
Landslide landform	10.01	4.64
Denuded slope landform	20.56	9.54
Headscarp, landslide, and denuded slope landforms	33.07	15.34
All of Seattle	215.59	100.00

the relative susceptibilities of the landforms to future landsliding. A table and graph on plate 1 shows these densities as the relative susceptibilities of each landform to future landsliding. The headscarp, landslide, and denuded slope landforms are denoted Zone 1, 2, and 3, respectively, on the plate. Also included on plate 1 is Zone 4, which covers the area of Seattle that was not mapped as headscarp, landslide, or denuded slope landforms (Zones 1–3).

The relative susceptibility values shown on plate 1 are meaningful when used to compare the susceptibilities of two or more zones or landslide types. For example, the table on plate 1 indicates total landslide susceptibilities of 122.2 and 0.5 for Zones 1 and 4, respectively. These values indicate that landslides are 122.2/0.5, or 244.4 times more likely within Zone 1 than Zone 4. As another example, in Zone 2, shallow and deep landslides have relative susceptibilities of 27.4 and 11.0, respectively; therefore, shallow landslides are 27.4/11.0, or 2.5 times more likely than deep landslides in this zone. In contrast, in Zone 1, shallow and deep landslides have susceptibilities of 83.1 and 14.8, respectively; therefore, shallow landslides are 5.6 times more likely than deep landslides in this zone.

As indicated in the table and chart on plate 1, landslide susceptibility decreases from Zone 1 (headscarp) to Zone 2 (landslide) to Zone 3 (denuded slope); susceptibility to landslides in Zone 4 is negligible. This trend is consistent for all classes of landslides with the exception of falls, for which Zone 3 shows a slightly greater susceptibility than Zone 2. It should be noted that the susceptibility values are indicative of potential landslide occurrence but not potential landslide travel paths. Thus, although the occurrence of long-runout landslides may be most likely in Zone 1, some that occur in this zone may travel downslope and pose significant hazards in other zones.

Table 3 provides the densities of historical landslides in terms of natural or human causation. As shown in the table, densities of human-caused landslides generally are much greater than densities of landslides that were caused solely by natural forces. The density trends among zones and landslide types apparent in table 2 also are apparent in table 3. For example, as in table 2, landslide densities in table 3 nearly always decrease from the headscarp landform to the landslide landform, and finally to the denuded slope landform. Human-caused landslides are extremely uncommon in the balance of Seattle area (Zone 4). Only four naturally caused landslides were reported in this area (Zone 4), which results in a spatial density of 0.01 that rounds off to 0.0 in table 3.

Table 4 provides ratios of the densities of human-caused landslides to the densities of landslides that occurred naturally. These ratios indicate the relative contribution of human activity in causing specific types of landslides on each of the landforms. The ratio of human-caused landslides generally increases as landslide density decreases on the landforms (tables 2 and 3). Thus, the less susceptible a landform to landslides, the greater the relative abundance of human-caused landslides on that landform and vice versa. This relation may suggest that slope-destabilizing human activities are more pronounced in areas that are considered less susceptible to landslides. In support of this explanation, Seattle has regulations specifically to address site investigation and development of zoned landslide-susceptible areas (many of which correspond to the LIDAR-mapped landforms), which should result in a reduction of slope-destabilizing activities and human-caused landslides within these areas. Additionally, public awareness of landslide hazards probably is greater in obviously susceptible areas where landslides often are reported so property owners probably are more careful that their activities do not destabilize slopes in these areas. Another possible explanation for the increased relative abundance of human-caused landslides with decreased landform susceptibility is the lower development density that exists in Seattle on steeper and presumably more susceptible slopes. Therefore, human activities are of greater density in areas less susceptible to landslides and vice versa. It seems likely that a combination of these factors, and perhaps others, is responsible for the greater abundance of human-caused landslides in areas that are less susceptible to landslides, in general.

Discussion

Plate 1 includes 173 landslides and landslide complexes, which is about 4 times more landslides than had been mapped previously in Seattle (Schulz, 2004). The plate also provides the first map of denuded slopes, which were largely formed by landslides. The potential usefulness of the landforms mapped on plate 1 for reducing landslide hazards in Seattle is indicated by evaluating the overall effectiveness of the landforms in capturing the locations of historical landslides. The landslide, headscarp, and denuded slope landforms capture 93 percent of

Table 2. Densities of reported historical landslides within the LIDAR-mapped landforms, Seattle, Washington.

Landform	Density of all landslides (landslides/square kilometer)	Density by landslide type (landslides/square kilometer)				Density of long-runout landslides (landslides/square kilometer)	Density by landslide size (landslides/square kilometer)	
		Deep	Fall	Shallow	Flow		Large	Small
Headscarp	122.2	14.8	9.2	83.1	10.4	22.8	23.2	93.5
Landslide	42.8	11.0	0.6	27.4	3.4	5.8	7.0	34.1
Denuded Slope	23.7	3.5	0.8	17.8	0.9	2.9	2.7	19.8
Balance of Seattle	0.5	0.1	0.0	0.4	0.0	0.0	0.0	0.4

Notes:

Meaningful comparisons of susceptibility values between the attribute fields of landslide type, runout characteristics, and size cannot be made. This is because each landslide has a value for each of these attributes; that is, each landslide is of a given type and size, and may or may not involve long runout.

Deep landslides extend to depths greater than 1.8 m (6ft); shallow landslides extend to depths less than 1.8 m (6 ft).

Long-runout landslides have greater than 15.2 m (50 ft) of runout.

Large landslides have areas greater than 930 sq. m (10,000 sq. ft); small landslides have areas less than 930 sq. m (10,000 sq. ft).

Table 3. Densities of reported historical landslides within the LIDAR-mapped landforms compiled on the basis of human or natural causes, Seattle, Washington

HUMAN-CAUSED LANDSLIDES

Landform	Density of all landslides (landslides/square kilometer)	Density by landslide type (landslides/square kilometer)				Density of long-runout landslides (landslides/square kilometer)	Density by landslide size (landslides/square kilometer)	
		Deep	Fall	Shallow	Flow		Large	Small
Headscarp	98.3	11.6	6.4	69.9	10.4	20.4	20.8	77.5
Landslide	35.2	9.7	0.3	21.9	3.3	5.4	6.4	28.6
Denuded Slope	20.2	3.3	0.6	15.5	0.7	2.6	2.4	17.7
Balance of Seattle	0.4	0.1	0.0	0.3	0.0	0.0	0.0	0.4

NATURAL LANDSLIDES

Landform	Density of all landslides (landslides/square kilometer)	Density by landslide type (landslides/square kilometer)				Density of long-runout landslides (landslides/square kilometer)	Density by landslide size (landslides/square kilometer)	
		Deep	Fall	Shallow	Flow		Large	Small
Headscarp	17.6	2.0	2.8	8.4	0.0	2.0	2.4	9.6
Landslide	5.3	0.7	0.3	3.8	0.1	0.3	0.3	4.0
Denuded Slope	2.2	0.2	0.1	1.2	0.1	0.1	0.2	1.1
Balance of Seattle	0.0	0.0	0.0	0.0	0.0	0.0	0.0	0.0

Notes:

Meaningful comparisons of susceptibility values between the attribute fields of landslide type, runout characteristics, and size cannot be made. This is because each landslide has a value for each of these attributes; that is, each landslide is of a given type and size, and may or may not involve long runout.

Deep landslides extend to depths greater than 1.8 m (6ft); shallow landslides extend to depths less than 1.8 m (6 ft).

Long-runout landslides have greater than 15.2 m (50 ft) of runout.

Large landslides have areas greater than 930 sq. m (10,000 sq. ft); small landslides have areas less than 930 sq. m (10,000 sq. ft).

Table 4. Ratios of densities of landslides with human causes to densities of landslides with natural causes, Seattle, Washington

Landform	All landslides	Deep landslides	Falls	Shallow landslides	Flows	Long-runout landslides	Large landslides	Small landslides
Headscarp	5.6	5.8	2.3	8.3	All HC	10.2	8.7	8.1
Landslide	6.6	13.9	1.0	5.8	33.0	18.0	21.3	7.2
Denuded Slope	9.0	17.0	4.0	12.7	7.0	26.5	10.0	15.8
Balance of Seattle	19.0	All HC	None	28.0	None	None	None	33.5
All of Seattle	7.4	13.3	2.4	8.9	24.7	16.4	12.4	10.2

Notes:

"All HC" indicates that all landslides with given characteristics reported on that landform were caused to some degree by human activity.

"None" indicates that no landslides with given characteristics were reported on that landform.

Deep landslides extend to depths greater than 1.8 m (6ft); shallow landslides extend to depths less than 1.8 m (6 ft).

Long-runout landslides have greater than 15.2 m (50 ft) of runout.

Large landslides have areas greater than 930 sq. m (10,000 sq. ft); small landslides have areas less than 930 sq. m (10,000 sq. ft).

all historical landslide locations in only 15 percent of the total map area. Virtually all (99.7 percent) naturally caused historical landslides occurred within these landform boundaries; all but four historical landslides that occurred outside of the mapped landform boundaries were caused by human activity. The better performance of the landforms in capturing the locations of natural versus human-caused historical landslides was expected because the mapped landforms are largely prehistoric features (Schulz, 2004). Therefore, the landforms were created largely by landslides that occurred naturally, while human activities can cause landslides virtually anywhere.

The conclusion that future landslide activity in Seattle will be similar to that of the past and concentrated within mapped landslide-related landforms is important to consider when evaluating the usefulness of plate 1 as a predictor of future landslide activity. Field investigations, LIDAR imagery, and historical records indicate that the landslides mapped on plate 1 are mainly complexes formed by many individual landslides, most of which were small and shallow and occurred prehistorically (Schulz, 2004). The same lines of evidence also indicate that headscarps and denuded slopes were similarly produced by many small, shallow, mainly prehistoric landslides. Nearly all historical landslides have been small and shallow, as well (Shannon & Wilson, Inc., 2003); hence, there has been no observable change in styles of landslide activity from prehistoric to historic times. The locations of landsliding in Seattle also have not varied from prehistoric time, as indicated by the capture of 99.7 percent of the locations of naturally caused historical landslides within the mapped, largely prehistoric landforms. Therefore, because historical landslide activity in Seattle has not noticeably varied from that of prehistoric time, it follows that future landslide activity will be of similar style and location. Consequently, the relative landslide susceptibilities shown on plate 1 should be indicative of future landslide activity.

Potential Uses of the Landslide Susceptibility Map

The landslide susceptibility map (pl. 1) identifies landslide-prone landforms within a large region with sufficient accuracy to permit recognition of general areas in which landslides may be expected. The map is not intended to replace site-specific engineering geologic and geotechnical investigations. As a regional-scale tool, the susceptibility map offers substantial benefits over previous susceptibility maps and Seattle zoning of landslide-susceptible terrain. Rather than defining only one area in which landslides are expected, as does current zoning, or general qualifiers such as "high" and "low" susceptibility as do many susceptibility maps, plate 1 provides variable, relative degrees of susceptibility to landslides in four zones. For example, as indicated in the table and chart of plate 1, Zone 1 is almost 3 times more susceptible to landslides than Zone 2, about 5 times more susceptible than Zone 3, and about 250 times more susceptible than Zone 4. In addition, plate 1 provides relative susceptibilities of the four zones to landslides with certain characteristics. This has the benefit of assisting implementation of appropriate landslide prevention efforts (such as described in Laprade and others, 2000) and municipal and public education efforts, since different landslide types often are caused by

different mechanisms and pose different hazards. For example, long-runout landslides are perhaps the most dangerous in Seattle because they occur with little or no warning, may travel significant distances from their initiation points at high speeds, and are capable of completely destroying buildings, as occurred recently on nearby Bainbridge Island when a family of four was killed in their home by a rapid long-runout landslide (Baum and others, 1998). These landslides are about 4 times more likely to initiate in Zone 1 than Zone 2, about 8 times more likely to initiate in Zone 1 than Zone 3, and are not expected in Zone 4. As another example, deep landslides typically are large and slow moving so rarely result in human casualties, but often result in significant property damage over a large area. For example, a deep landslide destroyed a roadway, utilities, and 4 homes (Shannon & Wilson, Inc., 2003) at the south end of Magnolia Bluff during 1996–98 (Baum and others, 1998). Deep landslides are about equally as likely in Zones 1 and 2, about 4 times more likely in these zones than in Zone 3, and unlikely in Zone 4 (pl. 1). This ability of the map (pl. 1) to identify and characterize susceptibility of the different zones (landforms) to different types of landslides can help focus and define appropriate landslide mitigation efforts in general and specific hazardous areas.

Human-Caused Landslides and Potential Uses of Tables 2 and 3

Improvements in identifying landslides and understanding their causative factors, as well as advances in geotechnical-engineering analyses and construction practices, should have resulted in a reduction through time of the proportion of Seattle's human-caused landslides. However, human-caused landslides still comprise the overwhelming majority, with more than 97 percent of historical landslides having a human contribution between January 2000 and August 2003, and more than 80 percent since 1980. Landslides in Seattle are caused primarily by changes in slope loading, strength, and ground-water conditions. Human activities that change slope loading and strength conditions include excavation into slopes, placement of fill onto slopes (including disposal of yard waste and other debris), and removal of vegetation, which provides strength to a slope through its root network when left in place (for example, Schmidt and others, 2001). Human activities that adversely affect ground-water conditions include poor surface grading that allows water to pond or be directed onto slopes, nonexistent or poorly performing curb-and-gutters surrounding pavements, highly permeable utility-trench backfill, leaking water and sewer pipes, undrained foundation systems that redirect and concentrate ground water, malfunctioning surface drainage systems (blocked inlets, culverts, etc.), improper routing of roof-drain systems (Baum and others, 2000), and removal of vegetation. Laprade and others (2000, Sections 6–9) describe methods to rectify these types of general problems and to reduce the potential for specific types of Seattle landslides. (Note that Laprade and others (2000) refer to shallow landslides as shallow colluvial landslides, falls as high bluff peeloffs, flows as ground-water blowouts, and long-runout landslides as debris flows.) Their study can be used to identify and address the factors contributing to human-caused landslides for specific areas of Seattle. The relative landslide hazards and degree of human causation of landslides within specific areas can be identified using tables 2 and 3 and plate 1. Of course, the most successful means of eliminating landslide hazards is avoidance of landslide-susceptible terrain, which is shown on plate 1.

Tables 2 and 3 provide information on landslide types, locations, and degree of human causation. The ratios in table 4 indicate the locations and types of landslides most likely to be caused by human activity. Higher ratios indicate a greater propensity for human-caused landslides. Table 4 indicates areas in which changes in human activity may have the greatest impact toward eliminating landslides. For example, all historical deep landslides and nearly all shallow landslides in the area outside of the LIDAR-mapped landforms (balance of Seattle area, Zone 4) and all flows on the headscarp landform (Zone 1) were caused to some degree by human activity (table 4). Efforts to reduce landslide hazards may be most successful for these types of landslides in these areas because they are virtually all partly caused by humans. The greatest overall reductions in city-wide landslide hazards may be most effectively achieved by identifying those areas that are highly susceptible to landslides using the densities on table 3, and also have high ratios of human-caused to natural landslides (table 4).

Conclusions

LIDAR imagery was used to map landslide, landslide headscarp, and denuded slope landforms throughout the city of Seattle. These landforms were created by numerous landslides that occurred since retreat of glacial ice at the end of the Pleistocene; nearly all of the landslides that created the mapped landforms are prehistoric features. Historical landslide occurrence also has been concentrated within the LIDAR-mapped landforms, as indicated by capture of 93 percent of the locations of over 1,300 historical landslides. The locations of virtually all historical landslides (99.7 percent) that occurred naturally are captured by the LIDAR-mapped landforms, even though the landforms only occupy 15 percent of Seattle's land area. Because of this concentration of historical landslides within predominantly prehistoric landforms, the spatial densities of historical landslides within each landform provide reasonable estimates of the relative susceptibilities of each landform to future landsliding. A relative landslide susceptibility map for Seattle was constructed based on these spatial densities and the landform map and indicates relative susceptibilities to landsliding based on landform and landslide type. Hence, the susceptibility map provides significantly more information regarding potential landslide activity than do conventional landslide susceptibility maps and should be a valuable tool for landslide hazard mitigation and reduction efforts in Seattle. The map is supplemented by ratios of human-caused to natural landslide susceptibilities, which indicate locations and types of landslides most prone to human causation and, thus, most likely mitigated by changes in human activity. Furthermore, the methods employed during this study for constructing the landslide susceptibility map should prove useful in similar

geologic environments where high-resolution topographic data and abundant historical landslide data are available.

References

Bates, R.L., and Jackson, J.A., 1987, Glossary of geology: Alexandria, Va., American Geological Institute, 788 p.

Baum, R.L., Chleborad, A.F., and Schuster, R.L., 1998, Landslides triggered by the winter 1996–97 storms in the Puget Lowland, Washington: U.S. Geological Survey Open-File Report 98-239, 16 p.

Baum, R.L., Harp, E.L., and Hultman, W.A., 2000, Map showing recent and historic landslide activity on coastal bluffs of Puget Sound between Shilshole Bay and Everett, Washington: U.S. Geological Survey Miscellaneous Field Studies Map MF-2346, 1 sheet.

Booth, D.B., 1987, Timing and processes of deglaciation along the southern margin of the Cordilleran ice sheet, *in* Ruddiman, W.F., and Wright, H.E., Jr., eds., North America and Adjacent Oceans During the Last Deglaciation; The Geology of North America, v. K-3: Boulder, Colorado, Geological Society of America, p. 71–90.

Booth, D.B., Troost, K.G., and Shimel, S.A., 2000, The Quaternary geologic framework for the city of Seattle and the Seattle-Tacoma urban corridor: U.S. Geological Survey Final Technical Report, 24 p.

Coe, J.A., Michael, J.A., Crovelli, R.A., and Savage, W.Z., 2000, Preliminary map showing landslide densities, mean recurrence intervals, and exceedance probabilities as determined from historic records, Seattle, Washington: U.S. Geological Survey Open-File Report 00–303, 25 p., 1 sheet.

Coe, J.A., Michael, J.A., Crovelli, R.A., Savage, W.Z., Laprade, W.T., and Nashem, W.D., 2004, Probabilistic assessment of precipitation-triggered landslides using historical records of landslide occurrence, Seattle, Washington: Environmental & Engineering Geoscience, v. X, no. 2, p. 103–122.

Cruden, D.M., and Varnes, D.J., 1996, Landslide types and processes, *in* Turner, A.K., and Schuster, R.L., eds., Landslides, Investigation and Mitigation, Transportation Research Board Special Report 247: Washington, D.C., National Research Council, p. 36–75.

Downing, John, 1983, The coast of Puget Sound; its processes and development: Seattle, University of Washington Press, 126 p.

Galster, R.W., and Laprade, W.T., 1991, Geology of Seattle, Washington, United States of America: Bulletin of the Association of Engineering Geologists, v. 28, no. 3, p. 235–302.

Gerstel, W.J., Brunengo, M.J., Lingley, W.S., Jr., Logan, R.L., Shipman, Hugh, and Walsh, T.J., 1997, Puget Sound bluffs: the where, why, and when of landslides following the holiday 1996/97 storms: Washington Geology, v. 25, no. 1, p. 17–31.

Hampton, M.A., Griggs, G.B., Edil, T.B., Guy, D.E., Kelley, J.T., Komar, P.D., Mickelson, D.M., and Shipman, H.M., 2004, Processes that govern the formation and evolution of coastal cliffs, *in* Hampton, M.A., and Griggs, G.B., eds., Formation, Evolution, and Stability of Coastal Cliffs – Status and Trends: U.S. Geological Survey Professional Paper 1693, p. 7–38.

Harp, E.L., Chleborad, A.F., Schuster, R.L., Cannon, S.H., Reid, M.E., and Wilson, R.C., 1996, Landslides and landslide hazards in Washington State due to February 5–9, 1996 storm: U.S. Geological Survey Administrative Report, 29 p.

Laprade, W.T., Kirkland, T.E., Nashem, W.D., and Robertson, C.A., 2000, Seattle landslide study: Shannon & Wilson, Inc. Internal Report W-7992-01, 164 p.

Miller, D.J., 1991, Damage in King County from the storm of January 9, 1990: Washington Geology, v. 19, no. 1, p. 28–37.

Montgomery, D.R., Greenberg, H.M., Laprade, W.T., and Nashem, W.D., 2001, Sliding in Seattle: test of a model of shallow landsliding potential in an urban environment, *in* Wigmosta, M.S., and Burges, S.J., eds., Land Use and Watersheds, Human Influence on Hydrology and Geomorphology in Urban and Forest Areas: Washington, D.C., American Geophysical Union, p. 59–72.

Mullineaux, D.R., Waldron, H.H., and Rubin, Meyer, 1965, Stratigraphy and chronology of late interglacial and Early Vashon glacial time in the Seattle area, Washington: U.S. Geological Survey Bulletin 1194–O, 11 p.

Paegeler, Margaret, 1998, Landslide policies for Seattle: A report to the Seattle City Council from the Landslide Policy Group: M. Paegeler, chair, 35 p.

Savage, W.Z., Morrissey, M.M., and Baum, R.L., 2000, Geotechnical properties for landslide-prone Seattle-area glacial deposits: U.S. Geological Survey Open-File Report 00-228, 5 p.

Schmidt, K.M., Roering, J.J., Stock, J.D., Dietrich, W.E., Montgomery, D.R., and Schaub, Timothy, 2001, The variability of root cohesion as an influence on shallow landslide susceptibility in the Oregon Coast Range: Canadian Geotechnical Journal, v. 38, no. 5, p. 995–1024.

Schulz, W.H., 2004, Landslides mapped using LIDAR imagery, Seattle, Washington: U.S. Geological Survey Open-File Report 2004-1396, 11 p., 1 plate.

Shannon & Wilson, Inc., 2003, Seattle landslide study update, addendum to the Seattle landslide study, stability improvement areas: Unpublished consultant report no. 21-1-08913-016 for Seattle Public Utilities, Seattle, Wash., 12 p.

Terich, T.A., 1987, Living with the shore of Puget Sound and the Georgia Strait: Durham, North Carolina, Duke University Press, 165 p.

Thorsen, G.W., 1989, Landslide provinces in Washington, *in* Galster, R.W., chairman, Engineering Geology in Washington: Washington Division of Geology and Earth Resources Bulletin 78, p. 71–86.

Tubbs, D.W., 1974, Landslides in Seattle: Washington Division of Geology and Earth Resources Information Circular 52, 15 p., 1 plate.

Tubbs, D.W., 1975, Causes, mechanisms and prediction of landsliding in Seattle: Seattle, University of Washington, Ph.D. dissertation, 89 p., 1 plate.

Wait, T.C., 2001, Characteristics of deep-seated landslides in Seattle, Washington: Golden, Colorado School of Mines, M.S. thesis, 131 p., 3 plates.

Waldron, H.H., 1967, Geologic map of the Duwamish Head quadrangle, King and Kitsap Counties, Washington: U.S. Geological Survey Geologic Quadrangle GQ-706, 1 sheet, scale 1:24,000.

Waldron, H.H., Leisch, B.A., Mullineaux, D.R., and Crandell, D.R., 1962, Preliminary geologic map of Seattle and vicinity, Washington: U.S. Geological Survey Miscellaneous Geologic Investigations Map I-354, 1 sheet, scale 1:31,680.

Youngmann, C. (ed.), 1979, King County: Coastal zone atlas of Washington: Olympia, Washington Department of Ecology, 9 sheets.

Yount, J.C., Minard, J.P., and Dembroff, G.R., 1993, Geologic map of surficial deposits in the Seattle 30’ by 60’ quadrangle, Washington: U.S. Geological Survey Open-File Report 93-233, 3 sheets.